



Nitrogen doped graphene-supported trimetallic CuNiRu nanoparticles catalyst for catalytic dehydrogenation of cyclohexanol to cyclohexanone

Alyaa K. Mageed^{a,b}, A.B. Dayang Radiah^{a,*}, A. Salmiaton^a, Shamsul Izhar^a, Musab Abdul Razak^a

^a Department of Chemical and Environmental Engineering, University Putra Malaysia, 43400 UPM Serdang, Selangor, Malaysia

^b Department of Chemical Engineering, University of Technology, Baghdad, Iraq

ARTICLE INFO

Article history:

Received 22 September 2017

Accepted 18 August 2018

Available online 19 August 2018

Keywords:

Cyclohexanol dehydrogenation

Copper catalyst

Tri metallic catalyst

Cu and Cu⁺ active sites

ABSTRACT

In different hydrocarbons reactions, copper based catalysts have industrial importance especially in the synthesis of the cyclohexanone from dehydrogenation of the cyclohexanol. At operating conditions, one of the significant problems in the industrial process is fast deactivation of the copper based catalysts. The present work focuses on the formulation of two types of the supported catalysts namely supported tri metals alloy (CuNiRu/N-rGO) in paper forms and supported copper (Cu/N-rGO), analysing the properties of the synthesised catalyst support (N-rGO) by Brunauer-Emmett-Teller (BET), X-ray photoelectron spectroscopy (XPS), Temperature-programmed desorption (TPD-NH₃), Temperature Programmed Reduction (TPR-H₂) and X-ray diffraction (XRD) as well as to investigate the catalytic performance of the two supported catalysts in the dehydrogenation of cyclohexanol to the cyclohexanone. All experiments on the catalytic performance were conducted at moderate temperatures (200–270 °C), 1 atm, 0.1 ml/min cyclohexanol flow rate and ~8 h time on stream (TOS). The performances of the catalysts were evaluated in the gas phase dehydrogenation of cyclohexanol to the cyclohexanone. The conversion of the cyclohexanol using CuNiRu/N-rGO is 4% higher compare to use of the Cu/N-rGO. The selectivity for cyclohexanone in case of the Cu/N-rGO catalyst is about 83.88%, whilst, the CuNiRu/N-rGO illustrated approximately 6% better performance. The yield of the cyclohexanone using the Cu/N-rGO is about 78%, while by adding the Ni and Ru as promoters with the improvement of the Cu/N-rGO the yield of cyclohexanone was improved by 8%. The duration of the steady state period significantly improved by using CuNiRu/N-rGO which was proposed up to 7 times. This research shows that the CuNiRu/N-rGO catalyst provides the suitable and selective active sites for the dehydrogenation of cyclohexanol to the cyclohexanone reaction.

© 2018 Production and hosting by Elsevier B.V. on behalf of King Saud University. This is an open access article under the CC BY-NC-ND license (<http://creativecommons.org/licenses/by-nc-nd/4.0/>).

1. Introduction

In the chemical industry, the catalytic dehydrogenation reactions are commonly used, and in the preparation of pharmaceuticals and fine chemicals, such reactions involving the oxygenated compounds are particularly important (Singh and Vannice, 2001). The main procedure for cyclohexanone production is the catalytic dehydrogenation of the cyclohexanol, which in the synthesis of pharmaceuticals and fine chemicals is an important intermediate.

* Corresponding author.

E-mail address: dradiiah@upm.edu.my (A.B. Dayang Radiah).

Peer review under responsibility of King Saud University.



<https://doi.org/10.1016/j.jksus.2018.08.007>

1018-3647/© 2018 Production and hosting by Elsevier B.V. on behalf of King Saud University.

This is an open access article under the CC BY-NC-ND license (<http://creativecommons.org/licenses/by-nc-nd/4.0/>).

For instance, producing of the caprolactam and adipic acid, the main raw materials in manufacture of the polyamide fiber in nylon textiles such as nylon-6 and nylon-6.6, respectively. Most of the uses of the caprolactam depend on the type and amount of impurities which it contains. In this case, higher purity requirements must be increasingly met by the raw materials (Simón et al., 2012a,b).

With catalysts based on the copper, cyclohexanol dehydrogenation processes are carried out as when they are carefully reduced, they present a highly dispersed copper phase. In this manner, they usually operate under mild conditions. Due to the copper sintering, these copper catalysts are not used at high temperature (Simón et al., 2012a,b). Recently, the field of alloy catalysts owing to their enhanced catalytic performance has been attracting a lot of interest compared to the individual components.

Because of the unique biological, electronic, optical, magnetic, and specifically catalytic properties, the metallic nanoparticles

(NPs) constructed from more than one metal have aroused great interest (Singh and Xu, 2013). In this case, owing to the interplay between electronic and lattice effects of the neighboring metals, multimetallic NP-based catalysts often show superior catalytic activities to their monometallic counterparts (Ataee-Esfahani et al., 2010). However, so far the controlled synthesis of the NPs consisting of multiple ($n \geq 3$) metal components has remained relatively unexplored and scientists have focused mainly on bimetallic systems (Wang and Li, 2011).

In order to enhance their properties, metals such as Rh (Mendes and Schmal, 1997), Co, Zn, Fe, Cr, Pd, Ni (Nagaraja et al., 2011) added to the copper catalysts. For catalytic activity of tri metallic catalysts, the shape and size distribution, surface segregation and crystalline structure, bulk and surface compositions are crucial factors (Ranga Rao et al., 2012).

On the other hand, as a low cost support for heterogeneous catalysts one can use a suitable support and type of interaction in industry with support material graphene to replace current metal oxide based catalyst supports, in order to maximize the catalytic activity of a catalyst (He et al., 2013). In this case, due to their high external surfaces, it is expected to be efficient, excellent high electrical conductivity and thermal/chemical stability which are leading to increase the selectivity and rate of the reactions, preventing poisoning and inhibition of sintering of the active metal surface by coke deposition (Julkapli and Bagheri, 2014).

This research focused on the formulation of the catalyst supported by nitrogen doped graphene (N-rGO) formulation of two different copper based supported catalysts (Cu, and tri metallic alloy CuNiRu), characterization by BET, XPS, TPR-H₂, TPD-NH₃ and XRD. For dehydrogenation of the cyclohexanol, testing the catalytic activity had been carried out for the two different catalysts to evaluate the role of the promoters (Ni and Ru), the effect of these two different catalysts on the activity and selectivity at different operating conditions (T = 200, 225, 250, 260 and 270 °C, P = 1 atm, liquid flow rate of reactant = (0.1 ml/min), gas flow rate of the carrier (N₂ gas) = 25 ml/min, and time of the reaction ~8h.

2. Methodology

2.1. Experimental

For unpromoted and promoted catalysts designated as CuNiRu/N-rGO and Cu/N-rGO, the dehydrogenation of cyclohexanol carried out. By Modified Staudenmaier's method, the Graphite oxide is prepared as reported by (Ambrosi et al., 2012); however, N-rGO was prepared as described in (Ning et al., 2013). Using incipient wetness impregnation of the Cu-precursor into the N-rGO support, the Cu/N-rGO catalyst was synthesised. The mass of the impregnated precursor was estimated to be equivalent to 1 wt% of the Cu. The N-rGO support was dried overnight at 110 °C, and the wet slurry containing the Cu-precursor (Cu(NO₃)₂·3H₂O, R&M chemicals) calcined and subsequently reduced for 3 h to obtain as-synthesised 1 wt%Cu/99 wt%N-rGO catalyst in a flow of N₂/H₂ (10% (v/v)) at 275 °C. In order to synthesise CuNiRu/N-rGO catalyst, the same preparation method of Cu/N-rGO catalyst was followed. The Cu-Ni-Ru-precursors (Ni(NO₃)₂·6H₂O, M. = 290.79 g/mole), (Cu(NO₃)₂·3H₂O, M. = 241.60 g/mole), and (Ru(NO)(NO₃)₃, M. = 317.09 g/mole) (R&M chemicals). The mass of the impregnated precursor was estimated to be equivalent to 0.5 wt%Cu, 0.25 wt% Ni and 0.25 wt%Ru.

Temperature programmed desorption using NH₃ (TPD-NH₃) was utilized to measure the acidity with temperature programmed reduction (TPR) studies of the catalysts were performed on a Thermo Finnigan TPDRO1100 series with 5% H₂-Ar as reducing and carrier gas. For specific surface area, by adsorption-desorption

isotherm using Brunauer-Emmett-Teller (BET method), all the catalysts were characterized using a Micromeritics Pulse Chemisorb 2700 instrument. Before measurements, the samples were oven dried at 393 K for 12 h and flushed in-situ with He gas for 2 h. As X-ray source operated at 25.6 W (beam diameter of 100 μm), the surface analysis of selected catalyst is carried out using the XPS (Ulvac-PHI, ULVAC-PHI Quantera II, INC.), with monochromatic Al-Kα (hν = 1486.6 eV). In this manner, the wide scan analysis was performed by using a pass energy of 280 eV with 1 eV per step. While, the narrow scan was performed using a pass energy of 112 eV with 0.1 eV per step. On a RIGAKU miniflex II X-ray diffractometer capable of measuring powdered diffraction pattern from 3 to 145° in 2θ scanning range, the XRD patterns of the catalysts in reduced forms recorded. The X-ray source is Cu Kα with wavelength (λ) of 0.154 nm radiation. In this case, the XRD has been set up with the latest version of PDXL, RIGAKU full function powder-diffraction analysis software.

2.2. Activity test

In a stainless steel fixed bed reactor Cyclohexanol dehydrogenation was carried out using a nitrogen gas cylinder which serves as the carrier gas and a liquid micro pump for feeding of the cyclohexanol into the reactor. Fig. 1 shows the schematic of the experimental set up. In this case, by external electric heater, the reactor was heated and insulated with glass wool. Using a K-type thermocouple, the temperature of the catalytic bed was monitored. Reaction was normally conducted under the following standard conditions: 200, 225, 250, 260 and 270 °C temperatures, 0.1 g catalyst weight, atmospheric pressure, 0.1 ml/min pure cyclohexanol feed flowrate, ~8 h reaction time.

Here, the reaction sequence was as follows: with the appropriate amount of catalyst, the reactor has been loaded. In order to run for 8 h under the above mentioned conditions, the reaction was allowed. In this case, by GC (Shimadzu 17A, FID, CP-Sil 24 CB 30 m 0.25 mm 0.25 μm), the Liquid samples were analyzed. The detected liquid products were as phenol and cyclohexanone. In case, the Gas analysis was performed in (Shimadzu 17A, TCD, HP-MoLesieve, 19095P-M50 30 m * 0.530 mm * 50 Mm) and the gaseous product was mainly hydrogen.

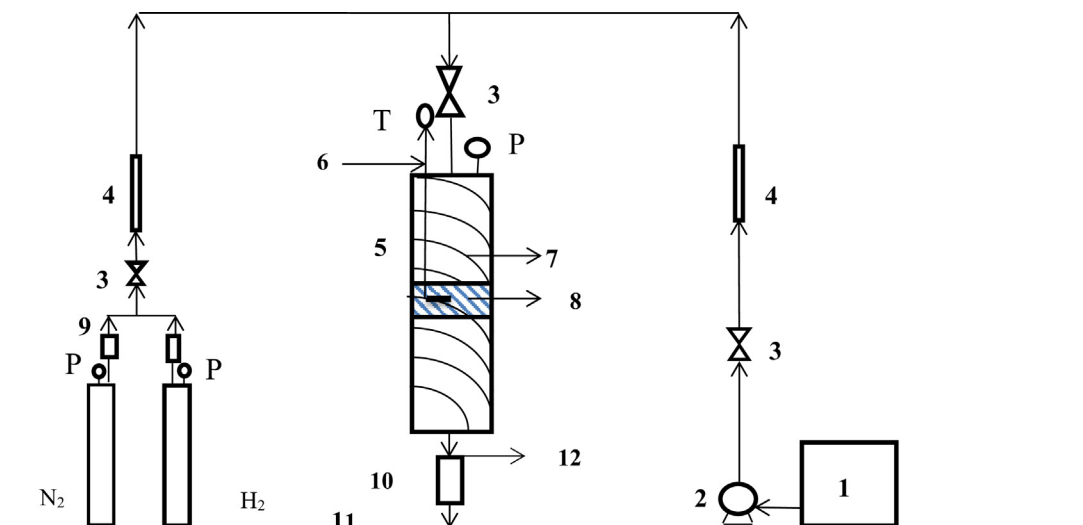
1: Liquid feed tank, 2: Liquid pump, 3: Valves, 4: Preheater, 5: Fixed bed reactor, 6: Thermocouple, 7: External electric heater, 8: Catalyst bed, 9: Rotameters, 10: Cooler, Gas-liquid separator, 11: Liquid sample and 12: Gas sample (H₂ gas).

3. Results and discussion

3.1. Characterization of the catalysts

3.1.1. BET

The heterogeneous catalysts are generally porous in nature. This characteristic plays an important role, in their catalysis application. The catalytic activity is closely linked to the available surface area for adsorption. The BET specific surface area, pore size and pore volume distributions of the CuNiRu/N-rGO and Cu/N-rGO samples analysed by the N₂ adsorption/desorption isotherms. For all of the classified samples, the N₂ adsorption-desorption isotherm (Balbuenat and Gubbins, 1993), in which two branches are almost parallel over a wide range of the P/P⁰ due to the IUPAC classification. For Cu/N-rGO and CuNiRu/N-rGO samples, the N₂ adsorption-desorption isotherm displaying the type-III isotherm (see Fig. 2(a and b)). Indeed, the samples have macroporous (pore size > 50 nm) structures. The Cu/N-rGO and CuNiRu/N-rGO samples have a hysteresis of the type H₃ according to the IUPAC classification. Attributed to the formation of the slit-shaped pores, these



1: Liquid feed tank, 2: Liquid pump, 3: Valves, 4: Preheater, 5: Fixed bed reactor, 6: Thermocouple, 7: External electric heater, 8: Catalyst bed, 9: Rotameters, 10: Cooler, Gas-liquid separator, 11: Liquid sample and 12: Gas sample (H₂ gas)

Fig. 1. Schematic of experimental set up.

samples have plate-like structures. Compare to that of the Cu/N-rGO catalyst, the CuNiRu/N-rGO catalyst recorded a decreasing about 90% in pores diameters and an increasing $\sim 75\%$ in the BET surface area (Table 1). Benefiting from the unique structure uniform distribution of the optimal size, the results imply that the Ni and Ru promoters provide a large surface area of the catalyst. In this way, with adding the different promoters such as Zn, Zr and Al, the improvement of the copper catalyst supported reduced graphene oxide (Fan and Wu, 2016). In this research, they found that by adding the promoters to the copper catalyst and the pore diameters decreased, the surface area of the catalyst would be enhanced.

3.1.2. TPD-NH₃

The NH₃-TPD analysis is used to measure the samples acidity. The quantitative estimation of the acidic site of the samples is summarized due to the desorbed amount of the ammonia (Table 2). Based on the peak temperature, in three different regions as 200–400 °C, 400–600 °C and above 600 °C, the results illustrate that the acidic sites are distributed. In this manner, the bimetallic Cu-Ni catalysts supported on the γ -Al₂O₃ was prepared by Pudi et al., (2015) and they stated that to the ammonia desorption from the weak acidic sites, the first region is attributed while the second region refers to the medium strength acidic sites. In case, from the strong acidic sites, the third region represents the ammonia desorption.

The desorption peaks at a range of medium acid sites illustrated by the CuNiRu/N-rGO and Cu/N-rGO catalysts. In this manner, the temperature at which the peaks desorption occurs related to the acidic strength. Table 2 shows that both of the CuNiRu/N-rGO and Cu/N-rGO and catalysts correspond to the medium acidic sites on their surfaces respectively with the NH₃ total amount desorbed of 4.64×10^3 and 2.57×10^4 $\mu\text{mol/g}$. In this way, suggested by the NH₃-TPD results, the addition of the promoters can change the total acidity and acidic strength of the catalyst surface. Ji et al. (2007) has been found to provide the suitable monovalent copper active sites based on the study of the dehydrogenation of the cyclohexanol over the Cu-ZnO/SiO₂ catalysts, the ZnO help as a

promoter. The total acidity of the trimetallic catalyst CuNiRu/N-rGO by 2.11×10^4 $\mu\text{mol/g}$ was higher than the Cu/N-rGO. However, the acidic strength is weaker than the Cu/N-rGO due to the rule of the promoter's Ni and Ru as encouraging increasing the activity of the catalyst and providing the suitable active sites as well.

3.1.3. XPS

The XPS is used more widely than the others to analyse the surface composition and oxidation states of the industrial catalysts. The photoelectron lines of the wide and narrow scan spectrum evidently present the Cu according to the XPS results as illustrated in Fig. 3. The metals loading in terms of the weight percent of the Cu to Ni and Ru and the loading of the CuNiRu alloy nanoparticles on the N-rGO support are close to the ratio of 50%:25%:25%. In case, it was found that due to the low content, there is no absorption peak of the Ni and Ru. Here, one can find the atomic percent (at%) of each of the elements for all the tested samples (see Table 3). From the atomic percentage results for the catalysts, the presence of the C, Cu, N and O in the sheets of the Cu/N-rGO and CuNiRu/N-rGO are proved.

Fig. 3 shows the high resolution spectrum of the Cu element. The peak at 933.2 eV is assigned to the Cu2p_{3/2} as per previous studies, which is attributed to either of the Cu and/or Cu₂O (Jia et al., 2015; Durando et al., 2008). Indeed, it is difficult to distinguish between these two species based on the Cu2p_{3/2} binding energies, as they are much close. Attributing to the binding energies of the Cu and/or Cu₂O, the CuNiRu/N-rGO catalyst illustrate the peak at 933.1 eV as well as the Cu/N-rGO. However, the peak shifted from the observed Cu2p_{3/2} of the CuNiRu/N-rGO catalyst. In this case, by the shift of the Cu2p_{3/2} binding energy, a strong electronic interaction between the Cu and Ni with the Ru elements in the metallic alloy are indicated.

3.1.4. H₂-TPR

The H₂-TPR usually is used to determine the reduction behavior of the catalysts. One can categorize the reduction behaviors of the CuNiRu/N-rGO and Cu/N-rGO catalysts into two stages of the reduction behavior (Fig. 4(a and b)). Due to the reduction behavior

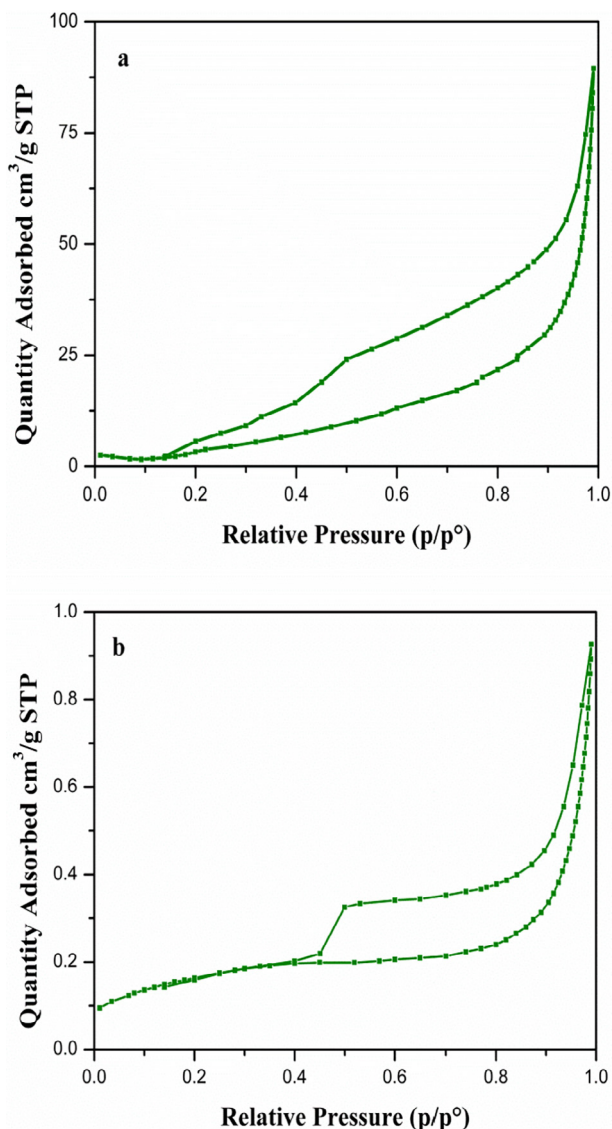


Fig. 2. Nitrogen adsorption-desorption isotherms of (a) Cu/N-rGO and (b) CuNiRu/N-rGO.

Table 1

Surface property for Cu/N-rGO and CuNiRu/N-rGO.

Samples	BET Specific surface area (m ² /g)	Pore volume (cm ³ /g)	Average pore diameter (Å)
Cu/N-rGO	7.44	0.11	874.17
CuNiRu/N-rGO	13.09	0.027	82.6

Table 2

Acidic Properties of the Fresh Cu/N-rGO and CuNiRu/N-rGO.

Samples	Amount of NH ₃ desorbed (μmol/g)			Total amount of NH ₃ desorbed (μmol/g)
	Weak	Medium	Strong	
Cu/N-rGO	–	4.64 × 10 ³	–	4.64 × 10 ³
CuNiRu/N-rGO	–	2.57 × 10 ⁴	–	2.57 × 10 ⁴

of the monovalent copper active sites (Cu₂O) to the metallic copper active sites (Cu⁰), based on the results reported by Bridier et al. (2010), the first stage of the H₂-TPR profile recorded at lower

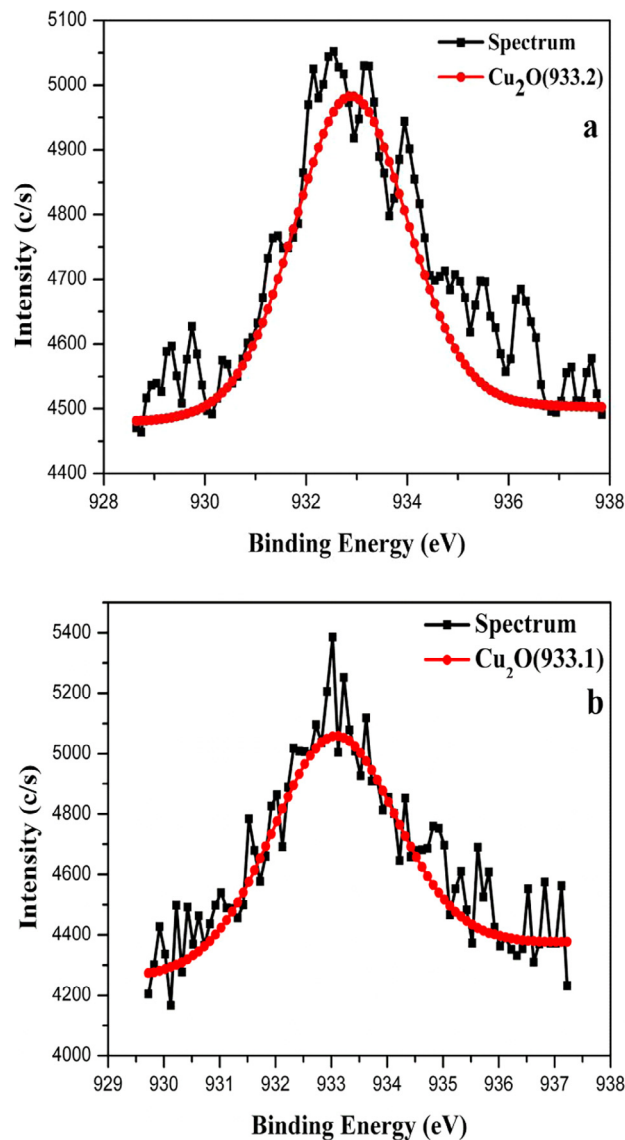


Fig. 3. XPS spectra of Cu₂p_{3/2} for (a) Cu/N-rGO and (b) CuNiRu/N-rGO.

Table 3

XPS results showing the atomic percent for each element of the samples.

Samples	C (at%)	O (at%)	N (at%)	Cu (at%)	Total (at%)
Cu/N-rGO	76.82	14.48	7.05	1.65	100
CuNiRu/N-rGO	75.81	14.71	8.71	0.77	100

temperature. In the case of the Cu/N-rGO and CuNiRu/N-rGO catalysts, as described in Schlapbach et al. (2001), the second peak possibly refer to the adsorbed H₂ on the C surface of the N-rGO. The CuNiRu/N-rGO catalyst comparing the Cu/N-rGO catalyst indicates decreasing about 18 °C in the reduction temperature. Due to the strong interaction between the Cu₂O species and the promoters' Ni and Ru causes highly dispersion of the copper active sites on the N-rGO support, the reduction temperature of CuNiRu/N-rGO catalyst could be shifted. In this case, the higher dispersion of the Cu₂O species responsible for their ease of reduction indicated by the shift clearly. In this way, in the study of the promoted copper catalysts, the results are in good agreement with the obtained results by Lin et al. (2010).

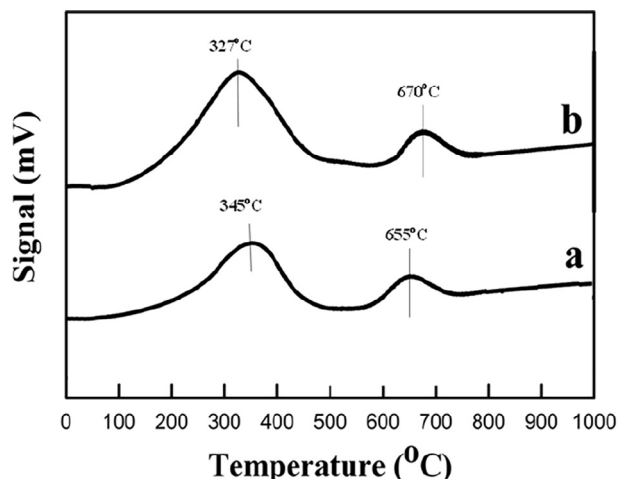


Fig. 4. H₂-TPR profiles of (a) Cu/N-rGO and (b) CuNiRu/N-rGO.

3.1.5. XRD

The crystallinity and phase determination of the samples were analyzed using the X-ray diffraction. Fig. 5(a and b) shows the XRD diffraction patterns of the Cu/N-rGO and CuNiRu/N-rGO where the XRD pattern of the Cu/N-rGO catalyst illustrates there are five diffraction peaks centered at $2\theta = 26.6^\circ$, 37.7° , 43.28° , 50.68° and 61.7° (Fig. 5(a)). In this case, the $2\theta = 37.7^\circ$, 43.28° and 61.7° might be indexed to the (1 1 1), (2 0 0) and (2 2 0) facets of the cubic phased Cu₂O (ICDD card number 00–001–1241) due to the surface oxidation of the Cu NPs, the first short and weak peak at $2\theta = 26.6^\circ$ can be attributed to the (0 0 2) planes of the N-rGO. However, the strongest peak can be attributed in the Cu/N-rGO pattern to the (1 1 1) facet of the Cu₂O. These findings are in good agreement with the results reported by Zhang et al. (2016) within providing the Cu₂O/rGO in one step of the reduced GO and loading the Cu₂O. The presence of the other phases of the copper interestingly indexed to the (2 0 0) confirming of the formation of the metal Cu and associated to the existence of the Cu crystallites detected at $2\theta = 50.6^\circ$. In this case, the crystallite size of the Cu₂O at $2\theta = 37.7^\circ$ of the (1 1 1) planes from Scherrer equation was estimated as 3.8 nm. In case, the presence of the Cu₂O and the metal Cu phases on the N-rGO support revealed by the XRD results.

Fig. 5(b) shows the XRD patterns of the CuNiRu/N-rGO catalyst. In this case, due to the presence of the amorphous carbon in N-rGO, the weak and broad peak at $2\theta = 26.7^\circ$ relates to the (0 0 2) planes.

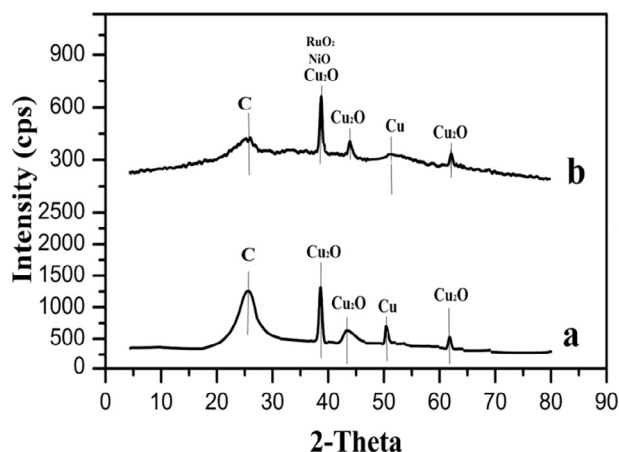


Fig. 5. corresponding XRD patterns of (a) Cu/N-rGO and (b) CuNiRu/N-rGO.

Attributed to the copper oxide (Cu₂O) for the (1 1 1), (2 0 0) and (2 2 0) planes, the diffraction peaks centered at $2\theta = 37.80^\circ$, 43.71° and 61.9° respectively. By the existence of the broad and weak diffraction peak at $2\theta = 50.6^\circ$, the presence of the metal Cu could be confirmed which can be indexed to the (2 0 0) planes. The peak at $2\theta = 37.80^\circ$ attributed to Cu₂O, NiO and RuO₂ respectively for (1 1 1), (1 1 1) and (1 0 1) planes. Compare to the Cu/N-rGO, this peak illustrates a slightly shift in angles to the higher value. The shift in the diffraction angle is due to the formation of the CuNiRu alloy as indicated by Bai et al. (2015) in their pioneering research on preparation of the hollow PdCu alloy supported on the N-rGO. Moreover, the crystal size of the CuNiRu/N-rGO catalyst estimated to be 1.13 nm which is smaller than those of the Cu/N-rGO about 2.67 nm. As an evidence for the existence of the CuNiRu/N-rGO catalyst in a strong interaction alloy one can consider the mentioned results.

The obtained results from the XRD diffraction support the H₂-TPR. As it is observed, the reduction behavior of the catalysts samples encourages one step reduction process due to the reduction of the Cu₂O (monovalent Cu⁺) to the Cu⁰ (metallic Cu). For the CuNiRu/N-rGO and Cu/N-rGO catalysts, from the XRD diffraction results the CuNiRu/N-rGO recorded the highly presence of the Cu₂O active sites and the smallest crystal sizes as well.

3.2. Catalytic cyclohexanol dehydrogenation

Figs. 6–8 illustrates the effect of the reaction temperature on conversion of the cyclohexanol over the CuNiRu/N-rGO and Cu/N-rGO catalysts and the cyclohexanone yields and selectivity. Here, the process temperature varies between 200 and 270 °C. In general, it is obvious that the cyclohexanol conversions the cyclohexanone yields (Figs. 6 and 7) and increases when the reaction temperature increases, while the selectivity of the cyclohexanone decreases at the same operating conditions (see Fig. 8).

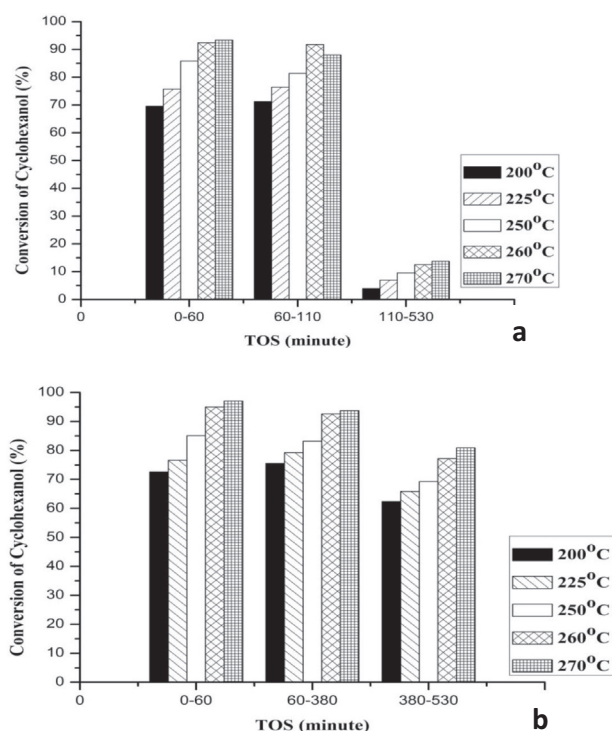


Fig. 6. Conversion of Cyclohexanol at different Time on stream (TOS) for (a) Cu/N-rGO and (b) CuNiRu/N-rGO.

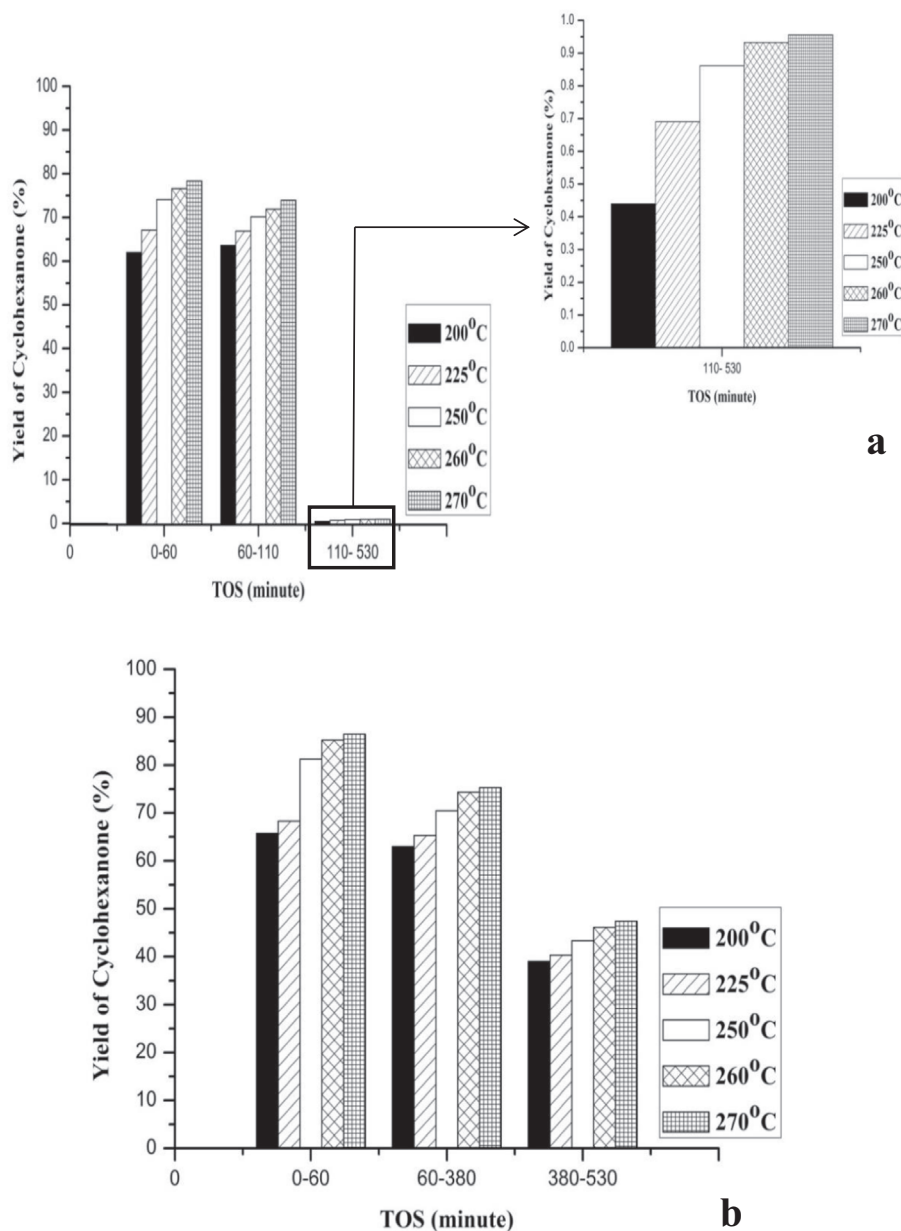


Fig. 7. Catalytic activities of catalysts in terms of yield of Cyclohexanone (a) Cu/N-rGO and (b) CuNiRu/N-rGO.

This is consistent with the activation energy trends for temperature dependent reactions, whereby the catalytic performance increases with respect to the temperature increasing in terms of the conversion of the reactants and the yield of the products (Smith, 2008). Compare to the catalyst Cu/N-rGO, the catalyst CuNiRu/N-rGO has an increase of 3.7% of the cyclohexanol conversion, 8.1% of the cyclohexanone yield, 8.8% of the cyclohexanone selectivity, at 270 °C and 60 min (Figs. 6–8).

As shown in Fig. 8, with rise of the temperature (200–270 °C), the cyclohexanone selectivity on both catalysts decreases. This can be due to the formation of the other by products e.g. phenol and cyclohexene via the side reactions occurring at the elevated temperatures such as the aromatization of the cyclohexanol to phenol and dehydration of the cyclohexanol to cyclohexene (Ji et al. (2007).

Not only for the reaction of the dehydrogenation of alcohol to the ketone the sites of the metallic copper are active sites but also for the reaction of aromatization of the cyclohexanol to the phenol.

Therefore, the metallic copper active sites are not selective. As indicated from the NH₃-TPD results, for this particular reaction, the CuNiRu/N-rGO is more suitable as within the actual dehydrogenation of the cyclohexanol to the cyclohexanone prefers the lower acidity active sites (Chang and Abu Saleque, 1993).

The stability of the Cu/N-rGO and CuNiRu/N-rGO catalysts was evaluated based on the times on stream (TOS) ~8 h (530 min). In this manner, the three different reaction stages can be identified as per Figs. 6–8, for the Cu/N-rGO as follows:

- For TOS = 0–60 min and reaction temperature 200–270 °C, the activation stage (Stage 1) shows increasing about 23.3% of the conversion of the cyclohexanol, 7% of selectivity of the cyclohexanone and 14% of yield of the cyclohexanone. The results' increasing is due to the activity of the fresh Cu/N-rGO catalyst.
- For TOS = 60–110 min Steady state stage (Stage 2) shows that the results are almost constant.

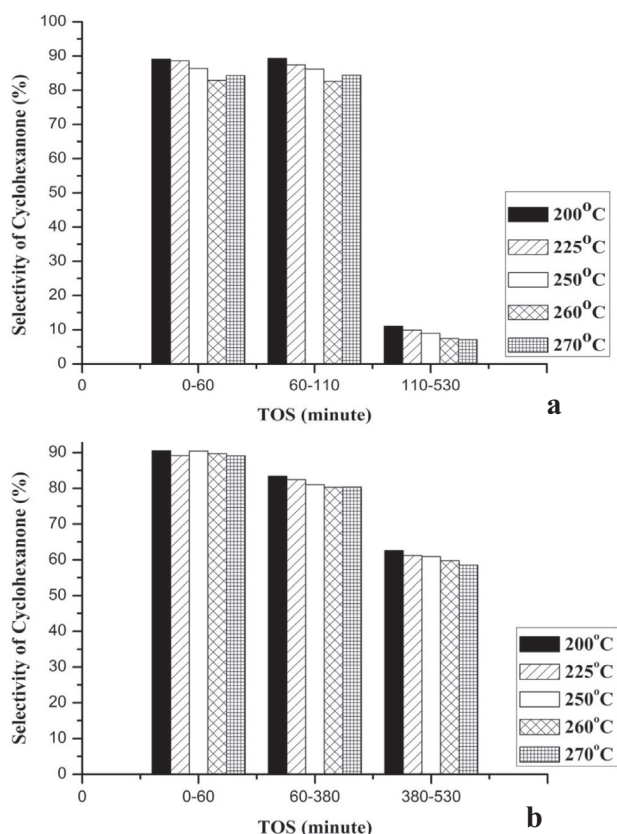


Fig. 8. Catalytic activities of catalysts in terms of selectivity of Cyclohexanone (a) Cu/N-rGO and (b) CuNiRu/N-rGO.

- The deactivation stage (Stage 3) shows a decline in the results for TOS = 110–530 min and reaction temperature 200–270 °C. The reduction in the results in terms of the reductive values between temperatures 200–270 °C as: the cyclohexanol conversion was about 10%, the selectivity of the cyclohexanone was 7%, yield of the cyclohexanone was 14%. The results suggest that the deactivation affects the reactions.

In this manner, one can identify the three different reaction stages for the CuNiRu/N-rGO as (see Figs. 6–8):

- The activation stage (Stage 1) shows increasing in conversion of the cyclohexanol for TOS = 0–60 min and reaction temperature 200–270 °C and selectivity and yield of the cyclohexanone. In this case, by the activity of the fresh CuNiRu/N-rGO catalyst the increasing in the results is caused.
- The steady state stage (Stage 2) shows that the results are almost constant for TOS = 60–380 min.
- The deactivation stage (Stage 3) shows a decline in the results for TOS = 380–530 min and reaction temperature 200–270 °C. In terms of reductive values of the temperatures 200–270 °C, in the results the reduction in the cyclohexanol conversion, yield and selectivity of cyclohexanone. Thus, by the deactivation based on the obtained results, the reactions slightly affected.

The Cu/N-rGO catalyst observed the decreasing of 67.1% of the cyclohexanol conversion, 46.4% of the cyclohexanone yield and 51.4% of the cyclohexanone selectivity. All the results support the idea of the fast deactivation of the Cu/N-rGO vigorously occurred after 110 min from the reaction started.

While, the CuNiRu/N-rGO catalyst has illustrated better stability at high TOS up to 380 min, and then a slightly reduced in the

results was observed up to the end of the reaction. Compared to that of the Cu/N-rGO in terms of increasing the reaction conversion the excellent CuNiRu/N-rGO performance and its stability at different TOS of the reactions could be attributed to the promotional effect of Ru and Ni in the formation of CuNiRu/N-rGO catalyst.

4. Conclusions

To investigate the catalytic performance of the supported catalysts in the dehydrogenation of cyclohexanol to cyclohexanone and to analyse the properties of the synthesised catalysts using TPD-NH₃, BET, XPS, TPR-H₂, TGA and XRD techniques, this research was revolved to formulate two types of the supported catalysts namely supported copper (Cu/N-rGO) and supported tri metals alloy (CuNiRu/N-rGO) in paper forms. The briefly conclusions from the major findings of this study are:

- The promoters (Ni and Ru) were added to the Cu/N-rGO catalyst and raised supervisor behaviors in terms of the provided suitable and selective active sites for catalytic dehydrogenation of the cyclohexanol to the cyclohexanone reaction with the smallest crystals size, higher thermal stability and larger surface area.
- The reaction results in terms of the highest cyclohexanol conversion, cyclohexanone yield and selectivity and hydrogen productivity in case of CuNiRu/N-rGO catalyst detected much improvement with in a reduction in phenol yield and selectivity as well.
- Due to the copper sintering, coke deposition and reduced active sites, the fastly deactivated in the Cu/N-rGO which might be. Thus, the CuNiRu/N-rGO has a much longer operational life. This is based on the performance evaluation of the catalysts.

Acknowledgement

This work was fully sponsored by the Ministry of Higher Education, Malaysia under the Fundamental Research Grant Scheme - (03-02-1522FR). All analyses, otherwise specified, were conducted at the Material Characterization Laboratory, Universiti Putra Malaysia.

References

- Ambrosi, A., Chua, C.K., Khezri, B., Sofer, Z., Webster, R.D., Pumera, M., 2012. Chemically reduced graphene contains inherent metallic impurities present in parent natural and synthetic graphite. *Proc. Natl. Acad. Sci.* 109 (32), 12899–12904.
- Ataee-Esfahani, H., Wang, L., Nemoto, Y., Yamauchi, Y., 2010. Synthesis of bimetallic Au@Pt nanoparticles with Au core and nanostructured Pt shell toward highly active electrocatalysts. *Chem. Mater.* 22 (23), 6310–6318.
- Bai, Z., Huang, R., Niu, L., Zhang, Q., Yang, L., Zhang, J., 2015. A Facile synthesis of hollow palladium/copper alloy nanocubes supported on N-doped graphene for ethanol electrooxidation catalyst. *Catalysts* 5 (2), 747–758.
- Balbuena, P.B., Gubbins, K.E., 1993. Theoretical interpretation of adsorption behavior of simple fluids in slit pores. *Langmuir* 9 (7), 1801–1814.
- Bridier, B., López, N., Pérez-Ramírez, J., 2010. Partial hydrogenation of propyne over copper-based catalysts and comparison with nickel-based analogues. *J. Catal.* 269 (1), 80–92.
- Chang, H.F., Abu Saleque, M., 1993. Dependence of selectivity on the preparation method of copper/ α -alumina catalysts in the dehydrogenation of cyclohexanol. *Appl. Catal. A* 103 (2), 233–242.
- Durando, M., Morrish, R., Muscat, A.J., 2008. Kinetics and mechanism for the reaction of hexafluoroacetylacetone with CuO in supercritical carbon dioxide. *J. Am. Chem. Soc.* 130 (49), 16659–16668.
- Fan, Y.J., Wu, S.F., 2016. A graphene-supported copper-based catalyst for the hydrogenation of carbon dioxide to form methanol. *J. CO₂ Util.* 16, 150–156.
- He, D., Jiang, Y., Lv, H., Pan, M., Mu, S., 2013. Nitrogen-doped reduced graphene oxide supports for noble metal catalysts with greatly enhanced activity and stability. *Appl. Catal. B* 132–133, 379–388.
- Ji, D., Zhu, W., Wang, Z., Wang, G., 2007. Dehydrogenation of cyclohexanol on Cu-ZnO/SiO₂ catalysts: The role of copper species. *Catal. Commun.* 8 (12), 1891–1895.

- Jia, Z., Chen, T., Wang, J., Ni, J., Li, H., Shao, X., 2015. Synthesis, characterization and tribological properties of Cu/reduced graphene oxide composites. *Tribol. Int.* 88, 17–24.
- Julkapli, N.M., Bagheri, S., 2014. ScienceDirect Graphene supported heterogeneous catalysts : an overview. *Int. J. Hydrogen Energy* 40 (2), 948–979.
- Lin, J.H., Biswas, P., Gulians, V.V., Misture, S., 2010. Hydrogen production by water-gas shift reaction over bimetallic Cu-Ni catalysts supported on La-doped mesoporous ceria. *Appl. Catal. A* 387 (1–2), 87–94.
- Mendes, F.M.T., Schmal, M., 1997. The cyclohexanol dehydrogenation on RhCu/Al₂O₃ catalysts: 2. chemisorption and reaction. *Appl. Catal. A* 163 (1–2), 153–164.
- Nagaraja, B.M., Padmasri, A.H., Raju, B.D., Rama Rao, K.S., 2011. Production of hydrogen through the coupling of dehydrogenation and hydrogenation for the synthesis of cyclohexanone and furfuryl alcohol over different promoters supported on Cu-MgO catalysts. *Int. J. Hydrogen Energy* 36 (5), 3417–3425.
- Ning, R., Tian, J., Asiri, A.M., Qusti, A.H., Al-Youbi, A.O., Sun, X., 2013. Spinel CuCo₂O₄ nanoparticles supported on n-doped reduced graphene oxide: a highly active and stable hybrid electrocatalyst for the oxygen reduction reaction. *Langmuir* 29 (43), 13146–13151.
- Ranga Rao, G., Meher, S.K., Mishra, B.G., Charan, P.H.K., 2012. Nature and catalytic activity of bimetallic CuNi particles on CeO₂ support. *Catal. Today* 198 (1), 140–147.
- Pudi, S.M., Biswas, P., Kumar, S. and Sarkar, B., 2015. Selective Hydrogenolysis of Glycerol to 1,2-Propanediol Over Bimetallic Cu-Ni Catalysts Supported on γ -Al₂O₃. *J. Braz. Chem. Soc.* [online], vol. 26, n. 8 [cited 2018–08–27], pp. 1551–1564. Available from: <http://www.scielo.br/scielo.php?script=sci_arttext%26pid=S0103-50532015000801551%26lng=en%26nrm=iso>. ISSN 0103-5053. <http://dx.doi.org/10.5935/0103-5053.20150123>.
- Schlapbach, L., Schlapbach, L., Züttel, A., 2001. for *Mobile Applications*, pp. 353–358.
- Simón, E., Pardo, F., Lorenzo, D., Santos, A., Romero, A., 2012a. Kinetic model of 2-cyclohexenone formation from cyclohexanol and 2-cyclohexenol dehydrogenation. *Chem. Eng. J.* 192, 129–137.
- Simón, E., Rosas, J.M., Santos, A., Romero, A., 2012b. Study of the deactivation of copper-based catalysts for dehydrogenation of cyclohexanol to cyclohexanone. *Catal. Today* 187 (1), 150–158.
- Singh, U.K., Vannice, M.A., 2001. Kinetics of liquid-phase hydrogenation reactions over supported metal catalysts – a review. *Appl. Catal. A* 213 (1), 1–24.
- Singh, A.K., Xu, Q., 2013. Synergistic catalysis over bimetallic alloy nanoparticles. *ChemCatChem* 5 (3), 652–676.
- Smith, I.W.M., 2008. The temperature-dependence of elementary reaction rates: beyond Arrhenius. *Chem. Soc. Rev.* 37 (4), 812–826.
- Wang, D., Li, Y., 2011. Bimetallic nanocrystals: Liquid-phase synthesis and catalytic applications. *Adv. Mater.* 23 (9), 1044–1060.
- Zhang, W., Li, X., Yang, Z., Tang, X., Ma, Y., Li, M., Hu, N., Wei, H., Zhang, Y., 2016. In situ preparation of cubic Cu₂O-RGO nanocomposites for enhanced visible-light degradation of methyl orange. *Nanotechnology* 27, (26) 265703.